Remote Sensing of Environment 141 (2014) 188–200

Contents lists available at ScienceDirect

Remote Sensing of Environment

journal homepage: www.elsevier.com/locate/rse

Mapping forest growth and decline in a temperate mixed forest using temporal trend analysis of Landsat imagery, 1987–2010

Chris J. Czerwinski *, Douglas J. King, Scott W. Mitchell

Carleton University, Department of Geography and Environmental Studies, Geomatics & Landscape Ecology Lab, Ottawa, Canada

ARTICLE INFO

Article history:
Received 19 March 2013
Received in revised form 26 October 2013
Accepted 9 November 2013
Available online xxxx

Keywords:
Landsat time-series
Forest change
Empirical modeling
Temporal trend analysis

ABSTRACT

Forest management seeks sustainability for a diverse set of goals, including economic objectives, provision of ecosystem services, and provision of a variety of possible land uses. It is important to quantify, map and monitor forest dynamics resulting from natural and anthropogenic processes over time periods appropriate to the temporal scale of change as well as to land management goals and decision making. This paper presents temporal trend analyses of temperate mixed forest dynamics in Gatineau Park, Québec, Canada, using a time series of Landsat 5 TM scenes. Several vegetation indices were first evaluated as indicators of field measured vegetation abundance parameters such as leaf area index, canopy openness, DBH, and basal area. Of these, Tasseled Cap Wetness (TCW) provided the best relationships (e.g., r = 0.81 against LAI) and it differentiated between coniferous, mixed and deciduous forests. Thirteen clear sky 5 TM scenes from the growing seasons of 1987 to 2010 were relatively calibrated and assembled into an image time-series. TCW applied to the image time-series followed by Theil–Sen and Contextual Mann–Kendall trend analysis detected subtle and gradual field-verified forest change. Gradual and abrupt forest decline or regrowth periods were identified; over the full period, 641 ha (1.8% of the park) exhibited statistically significant growth, and 689 ha (1.9%) exhibited decline. Mapping the timing, location, magnitude, and duration of forest change will help inform land management policy and actions within Gatineau Park and such methods may be applied in other similar forests.

1. Introduction

As a result of natural and human-induced disturbances and seasonal and successional dynamics, the structure and composition of a forest are constantly changing (Spies, 1998) at a range of scales in space and time (He et al., 2011). Understanding forest patterns, trends and rates is essential for their preservation and may help to assess the effectiveness of different management approaches (Paolini, Grings, Sobrinos, Munoz, & Karszenbaum, 2006).

Abrupt land cover conversions, such as a forest fire or clear cut, can often be detected using imagery of appropriate spatial resolution before and after the event (Gómez, White and Wulder, 2011). However, mapping and monitoring subtle vegetation dynamics such as longer-term decline, or growth, can require images from more than two dates, introducing additional challenges (He et al., 2011). This is mostly because variance in image data may be related to atmospheric variability, sensor calibration variability, image alignment, image processing or other environmental factors that can reduce the ability to detect image characteristics related to ecologically relevant change (Song, Woodcock, Seto, Lenney, & Macomber, 2001).

In the past, remotely detecting change was often limited by data availability, but using the Landsat satellite archive, which has recently become freely available, community-level forest monitoring has become increasingly feasible, and at a scale and cost that are meaningful from a management perspective. While bi-temporal change detection techniques provide valuable information about a landscape, if there is a wide interval between image dates, it can be difficult to interpret the timing or duration of a change detected. Early trend analysis using Landsat data often evaluated image calibration techniques, and found that for most applications, relative methods produce more temporally consistent time-series (Coppin & Bauer, 1994; Song & Woodcock, 2003). The challenge for forest trend analysis using remote sensing includes reducing the effects of the atmosphere, topography, phenology, and view angle (Song, Woodcock, & Li, 2002). Recent studies have confirmed that a Landsat image time series is capable of detecting subtle and abrupt inter-annual forest changes. Vogelmann, Tolk, and Zhu (2009) examined the Santa Fe National forest in New Mexico using a Landsat 5 TM image time-series comprised of 8 inter-annual image dates ranging from 1988 to 2006. Spectral trends starting in about 1995 showed a distinct increase in the short wave infrared/near infrared index, which they found to be highly correlated with canopy greenness and tree mortality. Severe tree mortality in their semi-arid study area was known to be a combined result of insect defoliation and drought. Powell et al. (2010) used Landsat data to model over 20 years of forest dynamics in both Arizona and Minnesota. Through

* Corresponding author.
E-mail addresses: c.j.czerwinski@gmail.com (C.J. Czerwinski), Dougj.King@carleton.ca (D.J. King), Scott.Mitchell@carleton.ca (S.W. Mitchell).

0034-4257/$ – see front matter © 2013 Elsevier Inc. All rights reserved.
http://dx.doi.org/10.1016/j.rse.2013.11.006

comparative efforts of several modeling approaches, they showed that no single modeling approach yielded the best results, and concluded that modeling errors are difficult to overcome at the pixel level (i.e. single date classification). They pointed out however, that the consistency of a Landsat image time series makes the relative changes potentially accurate, and recommended a linear approach to modeling ecological change.

1.1. Study area and research context

Gatineau Park (Fig. 1) is located in southern Québec, just north of Ottawa, Ontario within the Great Lakes-St. Lawrence Forest Region of the Canadian Shield (Pisaric, King, MacIntosh, & Bemrose, 2008). This 36,131 ha area comprises remnants of the Laurentian Mountains, now evident as rolling hills of igneous and metamorphic rock overlain by glacial deposits mostly comprised of till with pockets of clay in some stream valleys (NCC, 2005). The park's forests are a mix of deciduous and coniferous temperate and northern species. In the southern portion, sugar maple (*Acer saccharum*) dominates, however, pockets of American beech (*Fagus grandifolia*), trembling aspen (*Populus tremuloides*), and red oak (*Quercus rubra*) can be found. Other less dominant deciduous species include red maple (*Acer rubrum*), American basswood (*Tilia americana*), ironwood (*Ostrya virginiana*), white ash (*Fraxinus americana*), black ash (*Fraxinus nigra*), white birch (*Betula papyrifera*), and black cherry (*Prunus serotina*). In the northern part of the park, mixed and coniferous forests are more abundant, and include species such as the eastern white pine (*Pinus strobus*), eastern white cedar (*Thuja occidentalis*), eastern hemlock (*Tsuga canadensis*), white spruce (*Picea glauca*), and black spruce (*Picea mariana*).

Before 1960, mining and forest harvesting were common in the park and in the surrounding region (NCC, 2005). Subsequently, park management has favored conservation and recreation over industry, although multi-lane roads as well as house construction have continued to be permitted in various park locations. Forest change has also occurred in various areas of the park due to natural disturbances such as ice storms (King, Olthof, Pellikka, Seed, & Butson, 2005) and insect defoliation events (Louis, 2008). Ice storms, also known as glaze events, involve large amounts of freezing rain, which can cause significant damage to trees. A particularly large event occurred in the temperate regions of eastern North America in 1998. A long term research study was established in the park to model ice storm damage (King, Olthof, Pellikka, Seed and Butson, 2005) and subsequent composition and structure dynamics using high resolution airborne and satellite imagery. Related projects have mapped canopy deadwood distribution (Pasher & King, 2009), and developed multivariate models linking structural attributes to image derived variables (Pasher & King, 2010, 2011). However, no attempt has previously been made to map temporal trends in forest dynamics across the whole park on a time scale relevant to longer term management goals.

1.2. Research goal and objectives

The goal of this research was to identify and map gradients of forest ecosystem change throughout Gatineau Park over a period of about two decades, which corresponds well with the park's planning cycle. In this research, a change in vegetation abundance was considered to include changes in live green biomass resulting from either anthropogenic or natural factors. The research objectives were to:

1) Identify an appropriate image-derived vegetation index for use in temporal trend analysis based on evaluation of relationships for a variety of such indices with field measured estimates of vegetation abundance;
2) Map the location, direction (increase or decrease), timing and magnitude of spectral change within Gatineau Park's forests; and
3) Determine which vegetation communities are changing, the magnitude of change, and the inferred agents of change.

Landsat 5 Thematic Mapper (TM) imagery was used as described below because: i) it represents the most appropriate remotely sensed archival database for the required multi-decadal temporal scale; ii) the temporal archive is complete, meaning imagery has been acquired every 16 days over the whole period, and the archive is free (both of these in contrast to higher resolution satellite imagery); iii) the whole park is imaged within one scene, and; iv) the nominal ground pixel size of 30 m was deemed appropriate for forest patch level analysis while minimizing spatial variance in reflectance associated with tree species and micro site differences that would be present in higher resolution imagery. Objective 1 was addressed using field and Landsat 5 TM data from the growth season of 2010. For objective 2, the relationships identified in objective 1 were used to aid interpretation of trends extracted from the Landsat image time series. Objective 3 was addressed using corroborating evidence from field work and ancillary data available for the time period of this study.

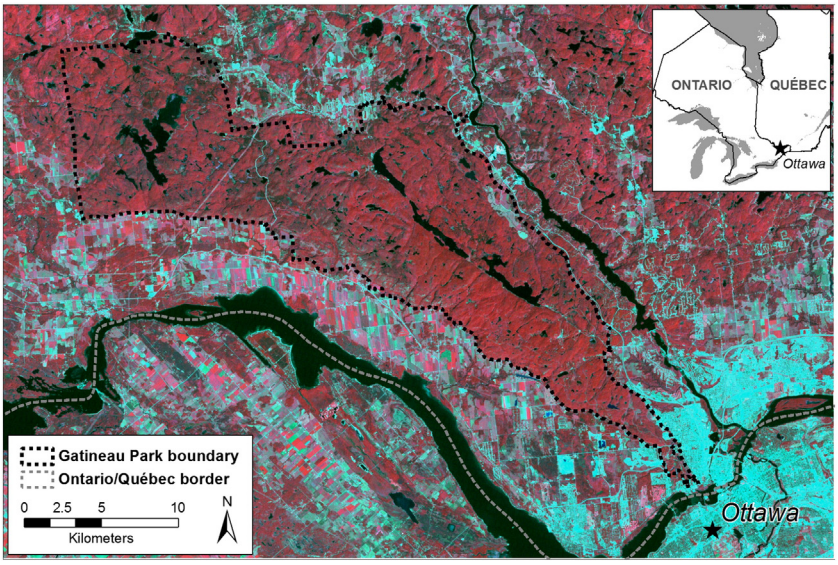

Fig. 1. Location of Gatineau Park, Québec, near Ottawa, Ontario, Canada. Shown using a color infrared composite of a Landsat 5 TM image acquired on August 9, 2004.

2. Methods

2.1. Field measurements

As a first step, existing Landsat imagery was used to identify potential field sites that represented the range of spectral trajectories associated with forest growth or decline. Image differencing of relatively calibrated (see Section 2.2) 1987 and 2007 normalized difference vegetation index (NDVI = [NIR-Red]/[NIR + Red]) images was conducted. Areas showing positive or negative change in NDVI ranging from small changes (about 1.0 standard deviation from the mean 1987–2010 difference) to large changes (greater than 2.0 standard deviations from the mean 1987–2010 difference) were selected as potentially subtle to severe vegetation change, respectively. Other areas showing no NDVI change were also selected to serve as control. The goal was to identify locations where growth, including normal height and volume growth in younger forest areas, or decline was occurring. Much of the forest of Gatineau Park is mature mixed deciduous, which was not expected to show significant growth or NDVI change over the 1987–2010 period. However, for management purposes, it was desirable to identify areas exhibiting regeneration and growth in areas that had been previously disturbed through anthropogenic land use or other processes.

Field confirmation was conducted and 33 plot locations were selected to represent a gradient of vegetation structure and composition conditions and dynamics. Plot locations were centered within areas that displayed near-homogeneous vegetation and topographic conditions over at least 150 m × 150 m (about 25 Landsat pixels). Plot size was 0.8 ha (90 m × 90 m), which corresponds to the approximate area covered by nine Landsat 5 TM pixels (i.e., a 3 × 3 pixel window). Plot corner positions were surveyed using a Trimble Juno GPS with expected horizontal accuracy of about 3–5 m, which is smaller than that of the image pixel size.

Field data were collected during leaf-on conditions in 2010. Hemispherical photographs acquired at 1.5 m height were used to estimate leaf area index (LAI) and canopy openness. LAI was calculated using the LX clumping index (which accounts for the non-random distribution of foliage elements in the canopy) described in Leblanc, Chen, Fernandes, Deering, and Conley (2005). For coniferous species, which are highly clumped, a needle-to-shoot ratio (g_E) multiplicative factor was used to refine these LAI estimates, using a weighting based on relative species abundance. These needle-to-shoot ratios were taken from the literature for white pine (1.91), black spruce (1.57) and balsam fir (*Abies balsamea*) (1.71; Chen, Govind, Sonnentag, Zhang, Barr & Amiro, 2006), red pine (*Pinus resinosa*) (2.08; Chen & Cihlar, 1995), white spruce (*Picea glauca*) (1.27; Hall, Davidson, & Peddle, 2003), Scots pine (*Pinus sylvestris*) (1.75; Gower, Kucharik, & Norman, 1999), and hemlock (1.65; Torontow & King, 2012). Some of these values were not derived in temperate forests of Gatineau park but they were the best available. The averages from five locations in each plot, acquired during the stable part of the growth season of 2010 (late July to end of August) were used as the main indicator of vegetation abundance. In addition to measurement of LAI and canopy openness, nine circular subplots (8 m radius) were used to measure the following 16 variables (for a total of 18 field variables): number of tree species; mean number of stems with DBH larger than 10 cm; mean live and dead DBH; mean overstory and sub canopy DBH; standard deviation of DBH (all trees); total, live, and dead basal area, mean age (using tree cores) of canopy trees, sub canopy trees, and all trees combined; mode of age of all trees; the cover of saplings greater than 2 m in height, and of all saplings measured on transects across each subplot. As some redundancy amongst the 18 field variables was expected, to determine a subset of non-redundant variables to model against the image based vegetation indices, Principal Components Analysis (PCA) was implemented. Components with eigenvalues greater than 1.0 (c.f. Kaiser, 1960) were retained and the variables most highly loaded on these components were used in empirical modeling against the image data (c.f. Pasher & King, 2010).

2.2. Satellite data and image processing

From the Landsat 5 TM archive, 13 summer scenes were available with less than 10% cloud cover for the years 1987 (08/11), 1989 (07/31), 1990 (08/19), 1994 (07/29), 1995 (09/02), 1999 (08/28), 2001 (08/01), 2002 (07/03), 2003 (08/23), 2004 (08/09), 2006 (07/30), 2007 (07/17), 2010 (09/11), where the numbers in brackets are month/day. The sequence of dates showed no trends with respect to vegetation phenology. The earliest within-season date was July 3 (2002), long after leaf-out (late May) and the latest was September 11 (2010). The latter was about 2–3 weeks before the onset of leaf color change and near the end of the period of stable LAI (Leblanc & Chen, 2001, for a similar forest about 60 km from the study area). Sun azimuth varied between 127 and 151° and sun elevation varied between 43 and 60°. These variations may have introduced small differences in brightness between images due to topography, which varied by about 150 m with slopes of up to about 30°. However, no corrections were implemented as relative calibration of the image time series as described below produced a very stable and low noise data set.

Experimentation with absolute calibration (using ATCOR2, Cos(t), and DOS, following Richter (1990), Chavez (1996), and Song et al. (2001), respectively), as well as relative calibration (Absolute-Normalization, Simple Regression and the PIF method, based on Schroeder, Cohen, Song, Canty, and Yang (2006), Song et al. (2001) and Schott, Salvaggio, and Volchok (1988)), to calibrate two images of the same growing season (August 3rd and 19th, 1990) showed that the relative calibration methods produced the most radiometrically comparable image data. Assuming negligible vegetation change between the two image dates, comparisons between calibration techniques showed that the differences of the means and standard deviations of the absolutely corrected image pairs were more than five times greater than all relatively corrected pairs. Also, for temporal analysis, relative methods were deemed to be suitable for the development of a calibrated image time series. Of the relative calibration methods tested, the PIF-based method (Schroeder et al., 2006) was selected and applied. Earlier studies such as Song et al. (2001) found that relative methods are generally most effective in establishing a radiometrically comparable image time-series. Schroeder et al. (2006) showed that the PIF method was slightly more accurate than that of other relative and absolute methods examined. Other studies have also shown the PIF method suitable for the development of Landsat image time-series for change detection (Du, Philippe, and Cihlar (2002)); Chen, Vierling, and Deering (2005); Paolini et al. (2006); Myeong, Nowak, and Duggin (2006)).

Twenty dark deep water targets and 20 bright quarry targets within 20–30 km of the park boundary were considered as PIFs and nine of each type were retained that had the most stable NDVI trajectories (Range of R^2 = 0.00022 to 0.06532; Range of slope = 0.00003 to 0.00101). The scene years selected as described above provided clear sky imagery over the park as well as over PIFs located outside the park. Their average pixel values in each band were then used to match band-specific image histograms to a master image using a linear transformation (Schott et al., 1988). The 2004 scene was used as the master because it displayed very high overall contrast amongst the brightness of the various land cover types in the scene, indicating that haze effects were minimal. To determine the noise level in the temporal image data set, post calibration residual variance not related to change was determined using five independent bright PIFs that had not been used in the relative image calibration above. For each PIF, the sum of the absolute slope and the standard error of the slope of its temporal trajectory were calculated. The five sums were averaged and this average was taken to be the minimum trajectory that could be considered to be potentially ecologically significant, i.e. not due to image-related noise. Since a linear calibration was used, residual noise was assumed to be primarily associated with non-linear atmospheric effects. This base noise level will hereafter be referred to as the 'noise floor'. Noise floor values were calculated for the vegetation indices (Section 2.3) used in this study; Section 3.2.2 presents the value for Tasselled Cap Wetness, which was found to be the best

indicator of temporal change as described in the Results. Image alignment errors were considered negligible for imagery with 30 m pixels, since each image showed a horizontal offset of less than 1 m when compared to the master image. Thus, image alignment procedures were not necessary. Lakes and wetlands were removed using a bitmap mask created from NCC vector data so that trends were based only on forested land cover. Clouds were manually removed from each image date and were treated as missing observations in time.

2.3. Extraction of vegetation indices and temporal trend analysis

NDVI was selected as one of the vegetation indices to be evaluated against the measured forest variables and for potential use in temporal trend analysis because of its known theoretical and empirical relationships with vegetation abundance and greenness (Goward, Markham, Dye, Dulaney, & Yang, 1991; Pettorelli et al., 2005; Wang, Adiku, Tenhunen, & Granier, 2005). However, where biomass is high, NDVI can be susceptible to saturation (Carson & Ripley, 1997; Turner, Cohen, Kennedy, Fassnacht, & Briggs, 1999); and where it is low, NDVI is affected by a strong background signal (Huete, 1988). Therefore, other spectral vegetation indices (SVI) were considered, such as the enhanced vegetation index (EVI), since it incorporates blue reflectance information to reduce signal noise and uncertainties, making it resistant to atmospheric influences (Jiang, Huete, Didan, & Miura, 2008) and the effects of forest structure (Chen, Vierling, Rowell, & DeFelice, 2004).

$$EVI = G\frac{P_n - P_r}{P_n + C_1P_r - C_2P_b + L} \quad (1)$$

where P_b, P_r, and P_n represent blue, red and NIR surface reflectance, respectively and G is a gain factor; C_1 and C_2 are aerosol resistance terms, and L is a soil-adjustment factor. Chen et al. (2004), used the suggested parameter values in Huete, Liu, Batchily, and van Leeuwen (1997); G as 2.5, C_1 and C_2 as 6 and 7.5 respectively, and L as 1. For sensors without a blue-band, EVI2 can be used (Jiang et al., 2008):

$$EVI2 = 2.5\frac{P_n - P_r}{P_n + 2.4P_r + L} \quad (2)$$

Landsat data are also commonly transformed using the Tasseled Cap transformation (Crist, 1985; Jin & Sader, 2005), which is a feature space rotation that reduces six bands to three orthogonal indices called brightness, greenness and wetness (TCB, TCG and TCW, respectively) (Healey, Cohen, Zhiqiang, & Krankina, 2005). These features of the Tasseled Cap transformation were also evaluated since they are often considered robust indicators of forest dynamics (Jin & Sader, 2005), using a linear combination of sensor-specific weightings for each band (Table 1), which are the original coefficients published for Landsat 5 TM brightness (DN) data.

All SVIs were calculated from image brightness (DN) data, testing showed the relatively calibrated time series to be much more stable and less noisy than reflectance calibrated data, as described in Section 2.2.

SVI data extracted from the Landsat imagery were averaged over the 9 pixels in each plot to derive a single value per plot. The SVIs derived from the 2010 Landsat imagery that showed the strongest correlations with one or more 2010 measured forest variables were selected for spatial and temporal analysis. Other metrics based on image spatial properties (e.g. texture) or spectrally unmixed fractions, which are sometimes related to vegetation structure and quantity metrics, were also evaluated but were not well related to the field data.

Coniferous, mixed and deciduous forests (hereafter referred to as functional groups) were stratified using vector data created in 1992 by the Quebec Ministry of Mines and Forests (QMMF) delineating homogenous forest patches based on age and species composition; these were useful for stratified modeling within each group. The NCC also provided spatial data describing the roads, trails, recreational facilities, and beaver monitoring sites within the park. Along with the rough insect defoliation sketch maps provided by the Quebec Ministry of Natural Resources and Fauna (QMNRF), these ancillary datasets were used to corroborate image analysis-based evidence of detected change.

Temporal analysis was implemented for three scale groups: the park as a whole, the three functional groups previously mentioned, and the plot-level. An initial evaluation of image differencing was used to detect abrupt changes in the park between two image dates. This method is widely used, and is therefore not the focus of this paper, but Czerwinski (2012) includes reports for a 2010 insect defoliation and a 2009 road built through the park. Temporal trend analysis over the image time series was conducted using methods adapted from Neeti and Eastman (2011) which combine the Theil–Sen (TS) Slope estimate and the Contextual Mann–Kendall (CMK) significance test. The TS slope, first proposed by Theil (1950) and later revisited by Sen (1968), provides an estimate of the median slope of all pair-wise iterations in the forward direction. For the CMK significance test for a monotonic trend, the null hypothesis (H_O) is that no trend exists (i.e. the data are independent of time, and are randomly ordered). It ranks all n(n-1)/2 pair-wise iterations in the forward direction. If the data value of a later observation is higher than an earlier observation, then the S statistic is incremented by 1. If the opposite scenario is true, S is decremented by 1 (Schlagel & Newton, 1996). The cumulative score of all pairs is used to calculate S:

$$S = \sum_{k=1}^{n-1}\sum_{j=k+1}^{n} sign\left(x_j - x_k\right) \quad (3)$$

where,

$$sign\left(x_j - x_k\right) = \begin{cases} +1 & if \quad x_j - x_k < 0 \\ 0 & if \quad x_j - x_k = 0 \\ -1 & if \quad x_j - x_k > 0 \end{cases} \quad (4)$$

where x_j and x_k are the annual values in years j and k, $j < k$, respectively. The variance of the S stat, in relation to the number of observations (n) in the time-series is used to determine a significance (p) value, which indicates the probability of obtaining a value greater than or equal to S, when no trend is present. The CMK significance test also incorporates spatial autocorrelation into the estimated p value, to take into account that neighboring trends (i.e. the trajectories of neighboring pixels) are likely to be similar. Details of integrating the TS and CMK tests can be found in Neeti and Eastman (2011).

The goal was to identify pixel locations associated with statistically significant vegetation index trends (positive or negative) over the time period of the study. Coupled with the 2010 data showing strong correlations between vegetation indices and field measured vegetation abundance (e.g., LAI), and based on the well-known theoretical relationships between image-based vegetation indices and vegetation abundance (summarized earlier in this section), such significant temporal trends in a given VI could be justifiably interpreted as changes or trends in vegetation abundance. For such non-parametric techniques, relatively small sample sizes can be used (Neeti & Eastman, 2011). Given that the maximum number of observations for any pixel location for this study was 13 (image dates), this was considered beneficial to the analysis. According to Hoaglin, Mosteller, and Tukey (2000), 29% of the observations included in the TS slope estimate can be in error, without affecting the estimated slope. For this research, the pixels with significant monotonic temporal trends ($p \leq 0.05$) as identified by the CMK analysis, and with

Table 1
Band-specific weights for each Tasseled Cap feature (Crist & Cicone, 1984).

Tasseled Cap feature	Weighting for Tasseled Cap transformation using Landsat 5 TM data					
	TM1	TM2	TM3	TM4	TM5	TM7
Brightness	0.3037	0.2793	0.4343	0.5585	0.5082	0.1863
Greenness	−0.2848	−0.2435	−0.5436	0.7243	0.0840	−0.1800
Wetness	0.1509	0.1793	0.3299	0.3406	−0.7112	−0.4572

TS slopes greater than the noise floor of a particular SVI, were mapped as positive or negative gradual change.

As an initial investigation the entire image time series, representing growth seasons from 1987 to 2010, was analyzed. However, it was necessary to remove the 2010 image because severe insect defoliation in the southern portion of the park resulted in many pixels being extreme negative outliers. The significance of a trend, calculated by the CMK test, is based on the number of iterations in the forward direction that demonstrate a particular direction of change compared to the total number of possible iterations in the time series. If the final observation in the series is extremely negative compared to the previous positive trend observations, then the true direction of change may be misinterpreted, and the resulting S-stat value may cause H_0 to not be rejected, falsely missing a longer term positive trend.

Following the above analysis of trends over the full 20 year period, two additional analyses were performed to investigate the sensitivity of the detected trends to the length of the temporal data set and the monitoring interval. To test the effects of the length of the temporal data set, the start and end years of the time series were modified to reduce the total temporal period. Two 17 year subsets of the twenty year Landsat data were produced by dropping data at the end and beginning of the time series. This produced data sets for the periods 1987 to 2004 and 1990 to 2007, respectively. Using this method, a reduction in three years from a 20 year time series to 17 years was deemed to be suitable to test whether the end points in the original 20 year series were responsible for the trends detected or if the trends were present over a shorter time period. Also, change pixels highlighted in most or all of these slightly different temporal data sets were considered to be the most reliable indicators of change locations within the park.

The second test of effects of time interval between images on detected trends was implemented by removing certain years' data within the image time series. In the original 20 year data set, the interval between Landsat images was 1–3 years, with the exception of two 4-year intervals. Two new time series were produced with consistent but longer time intervals between sample years by dropping data from certain years. The first data set had a 4- to 5-year interval (1987, 1990, 1994, 1999, 2003, 2007), and the second had a 6- to 7-year interval (1989, 1995, 2001, 2007). The goal of this test was to determine if the trends detected in the original 20 year data set could be detected using longer intervals between images. If so, it would mean the trends detected are not highly sensitive to the monitoring frequency.

Validation of the trends found within the 20-year TCW time series was conducted using a set of additional randomly selected sites not used in trend modeling. Thirty sites were selected from areas in the trend map highlighted as significant positive change and 30 more sites were selected from areas in the trend map highlighted as significant negative vegetation change. These sites were then visited during the stable part of the growth season of 2011 and the conditions visible within a radius of at least 20–30 m were noted in relation to the trends detected in the time series. This sampling process is equivalent to testing user's accuracy or errors of commission as sites representing positive and negative change in the trend map were selected and then field validated.

3. Results

3.1. Field data analysis and relationships with vegetation indices

PCA results using 18 field variables derived from the 2010 scene showed that the first six PCs were significant (eigenvalues > 1.0 (c.f. Kaiser (1960)) and cumulatively explained 88% of the variance of the original dataset. Varimax rotation (Kaiser, 1958) was then implemented on the resulting components to maximize the sum of the variances of the squared variable loadings and produce a simpler structure where variable loadings are high on one or a few components and very low on others. The field variables with the highest factor loadings on these PCs were used in correlation analysis against the SVIs selected for this research. TCW and EVI2 revealed the strongest correlations. For example, EVI2 was negatively correlated with the average number of stems ($r = -0.61$, $p \leq 0.001$) and canopy openness ($r = -0.57$, $p \leq 0.001$) while TCW was strongly correlated (Fig. 2) with LAI ($r = 0.81$, $p \leq 0.001$). Fig. 2 shows a distinct gradient among the functional groups from low LAI deciduous plots through moderate LAI mixed plots to high LAI coniferous plots.

When considering each functional group independently, TCW showed the greatest number of significant and strongest relationships with the field data. Field variables that formed significant models with TCW or EVI2 ($r > 0.60$, $p < 0.1$) for any of the functional groups included average number of stems, standard deviation of DBH, average age of sub-canopy tree species, average DBH of standing dead trees, canopy openness, and average live basal area. In some cases, EVI2 and TCW produced conflicting results. For example, Fig. 3 shows a map of a red pine plantation (outlined in brown) represented by EVI2 and TCW, respectively, that highlights this conifer-dominated region as an area of either low (EVI2) or high (TCW). The field measured LAI in this plantation was amongst the highest of all plots sampled, suggesting that TCW is a more reliable indicator of vegetation abundance for this region of the park. Seed and King (2003) discuss how the canopy architecture of a coniferous forest produces darker shadows than deciduous forests that may affect the value of a SVI; this may be why EVI2 is lower for this plantation. Both EVI2 and TCW are well founded indicators of vegetation abundance, but they represent differing signal responses. EVI2 is a vegetation index founded on reflectance theory (Section 2.3), while TCW is an index of moisture content (which is higher in more dense vegetation canopies) that is based on a rotation of spectral feature space and was developed using empirical data (Section 2.3). Neither was considered superior to the other based on theoretical foundation nor previous empirical results in the literature, however, based on the observations described above and the higher correlation of TCW with LAI, TCW was deemed to be a stronger indicator of vegetation abundance at our site.

3.2. Temporal analysis

3.2.1. Analysis of plots observed in the field to be growing or deteriorating in 2010

Plots observed in the field to be regenerating or deteriorating were appropriately modeled over time by either EVI2 or TCW, but in most cases, TCW showed a stronger trajectory as represented by lower residuals about the trend line (Fig. 4). Further comparisons were made between both image variables from a temporal perspective, but are not reported here (see Czerwinski, 2012). Based on these analyses, TCW

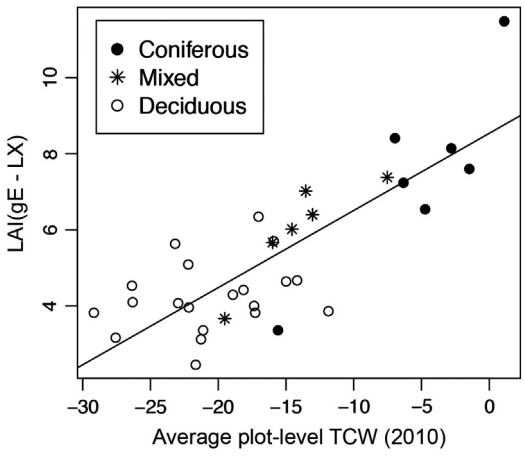

Fig. 2. Significant bivariate regressions between LAI of all plots ($n = 33$), and their respective mean TCW values derived from 9 pixels in each plot. LAI values include the clumping index and, for coniferous species, a needle-to-shoot ratio (g_E) refinement as described in Section 2.1.

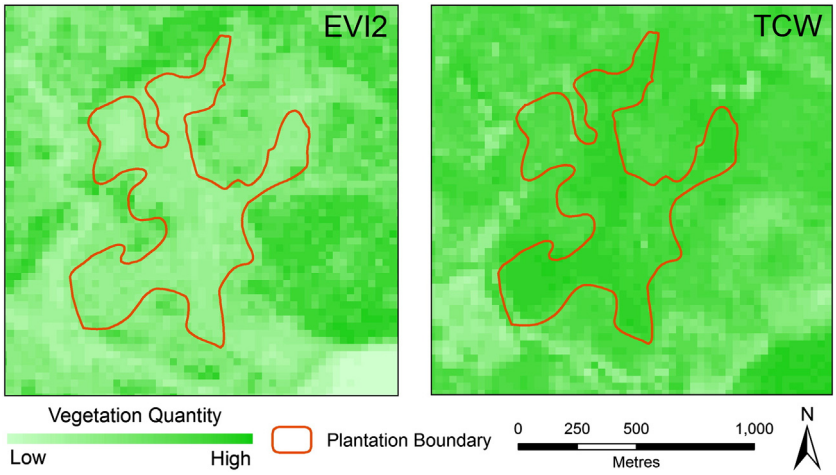

Fig. 3. A coniferous plantation of high LAI misrepresented as lower vegetation abundance by EVI2 and correctly represented as higher vegetation abundance by TCW.

was selected as the main indicator of vegetation abundance for the remainder of the temporal analysis.

3.2.2. Trend analysis

A pixel's temporal trajectory was considered representative of persistent and cumulative vegetation change if its TS slope estimate was greater than the TCW noise floor (+/- 0.36), and if based on the results of the CMK significance test, the null hypothesis of no change could be rejected. From Fig. 2, this noise floor represents about 1.2% of the range of sample TCW data and much less than 1 unit of LAI, indicating that the relatively calibrated time series was very stable with low noise. The following analyses present temporal trends that met both the CMK and TS criteria.

3.2.2.1. 1987–2007 trend analysis. Trend analysis was conducted using all TCW images, with the 2010 TCW image removed due to the short term defoliation event as described in Section 2.3. This produced clearer trends over the twenty years from 1987 to 2007 ($n = 12$), referred to hereafter as the 20-year time series. The results highlighted about 995 ha and 549 ha as significantly decreasing and increasing in vegetation abundance, respectively over these 20 years (Fig. 5).

The results of this time-series analysis not only allowed for the ability to map the direction of change, the magnitude of an event was also interpreted by thresholding the slopes of each trajectory identified by the Theil–Sen analysis. Pixels with a TCW trajectory slope greater than 2 times the noise floor (NF = +/−0.36) were assigned to one of three classes: low (trajectory slope = 2 to 4 × NF), moderate (trajectory slope = 4 to 6 × NF) and high (trajectory slope > 6 × NF). These mapping criteria were used to allow comparisons by separating extreme trajectories (high slope over time) from more subtle trajectories (lower slope over time), while ensuring the latter were still highly significant (greater than 2 × NF). From a management perspective, this stratification could be used to identify priority regions for interventions.

Fig. 6 illustrates two locations in the park that showed a significant negative change trajectory over the 20-year time series (outlined in black), and it includes a map describing the trajectory slope class of each pixel within that area. It can be seen that region 'B' has pixels associated with all three trajectory classes, whereas region 'A' is associated with only the low trajectory slope class. Region 'B' has changed more during the given time period, and the most severe change has occurred in the center of the delineated area. The results in Fig. 6 are not surprising; in the field, region 'B' was observed to be in a state of severe decline since it was largely comprised of standing dead trees. Region 'A' was obviously in a state of decline, but had a much larger proportion of standing live trees. Both areas were correctly detected as undergoing a long term reduction in vegetation abundance.

3.2.2.2. Sensitivity of trend analysis results to start and end dates. The sensitivity of the above trend analysis results to the beginning and end dates of the series was evaluated by producing two new 17-year series, the first, 1987 to 2004 with an earlier end date and the second, 1990 to 2007 with a later start date. Hereafter, these are referred to as the early- and late-17 year time series, respectively, each being comprised of 10 TCW images. Table 2 provides a summary of the area found to have

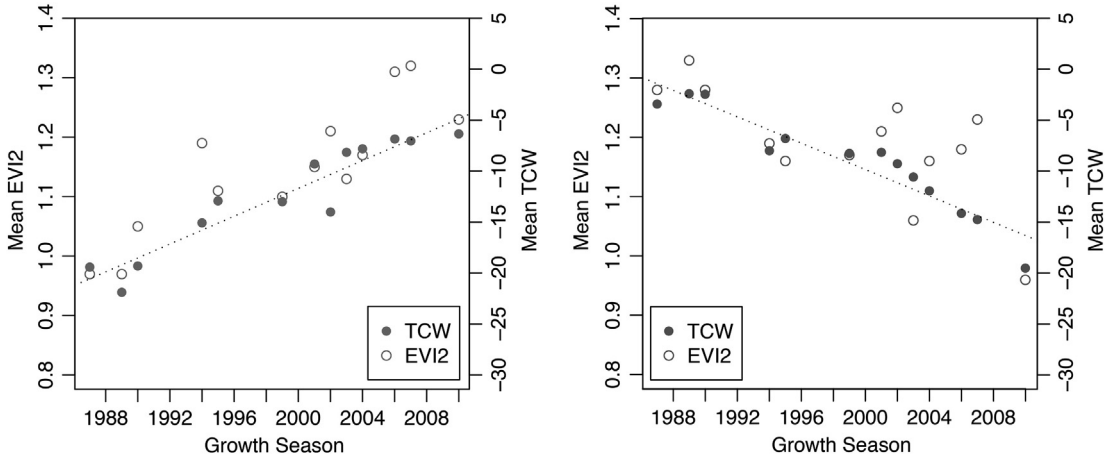

Fig. 4. EVI2 and TCW plot-level trajectories of a growing forest (left) and deteriorating forest (right).

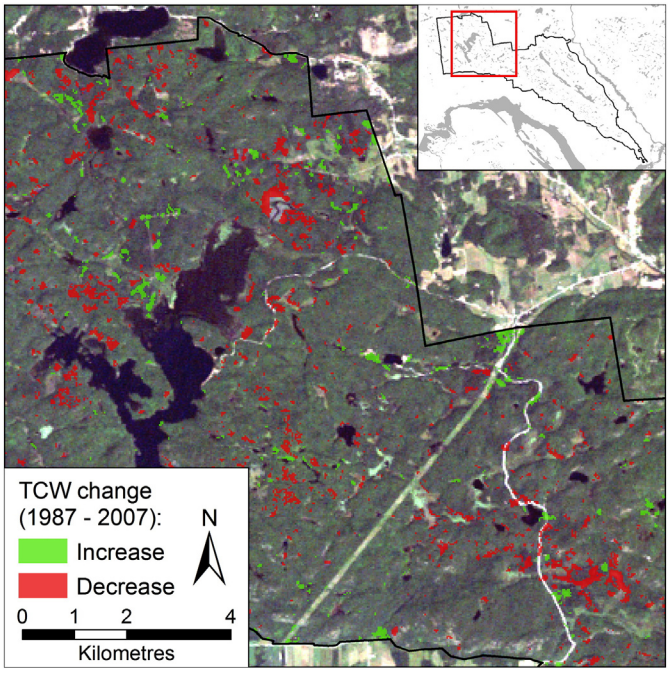

Fig. 5. Results of the trend analysis using all images available (1987 to 2007) for a portion of Gatineau Park (inset). Areas highlighted in red and green represent significant negative and positive spectral trajectories, respectively (i.e., trajectory slope > noise floor; $p \leq 0.05$). (For interpretation of the references to color in this figure legend, the reader is referred to the web version of this article.)

significantly changed for the two 17-year data sets and the 20-year data set. The total areas of positive and negative change found for each of the three temporal data sets are quite different. The total area identified as having undergone significant spectral change in each data set is also small in relation to total park area; i.e. as expected, the park's forest cover is not deteriorating overall, but there are local areas where change is significant.

Table 2
Area (ha) of significant ($p \leq 0.05$) positive and negative TCW change for three different time series analyses.

Time period	Observations (n)	Significant positive TCW change		Significant negative TCW change	
		Area (ha)	% of park	Area (ha)	% of park
1987 to 2007	12	549	1.5	995	2.7
1987 to 2004	10	1021	2.8	394	1.1
1990 to 2007	10	352	1.0	679	1.9
Average	11	641	1.8	689	1.9

Fig. 7 shows two prominent forest areas where vegetation had ongoing decline in 2010. Losses appeared to be a result of surface hydrology conditions (saturated soils and probably beaver-induced flooding). Both locations were identified using the 20-year and both 17-year time series, thereby providing spectral and statistical evidence of persistent and gradual change. The spatial distribution of predicted change is notably different, but the same general area is being targeted as deteriorating for all three time series. The early 17-year time series (yellow outlines) appears to show the least amount of change, and as later observations are included in the analysis, the area of change increases.

3.2.2.3. Sensitivity of trend analysis results to time interval between images. TCW time series were assembled with a longer average time interval between observations than the 1–3 years of the 20 and 17-year series above. This provided additional information on the appropriate observation frequency for detection of the identified forest trends in the park. A 4–5 year interval produced similar change results as the 1–3 year interval of the time series above, however, the 6–7 year interval did not result in successful detection of the same changes: it

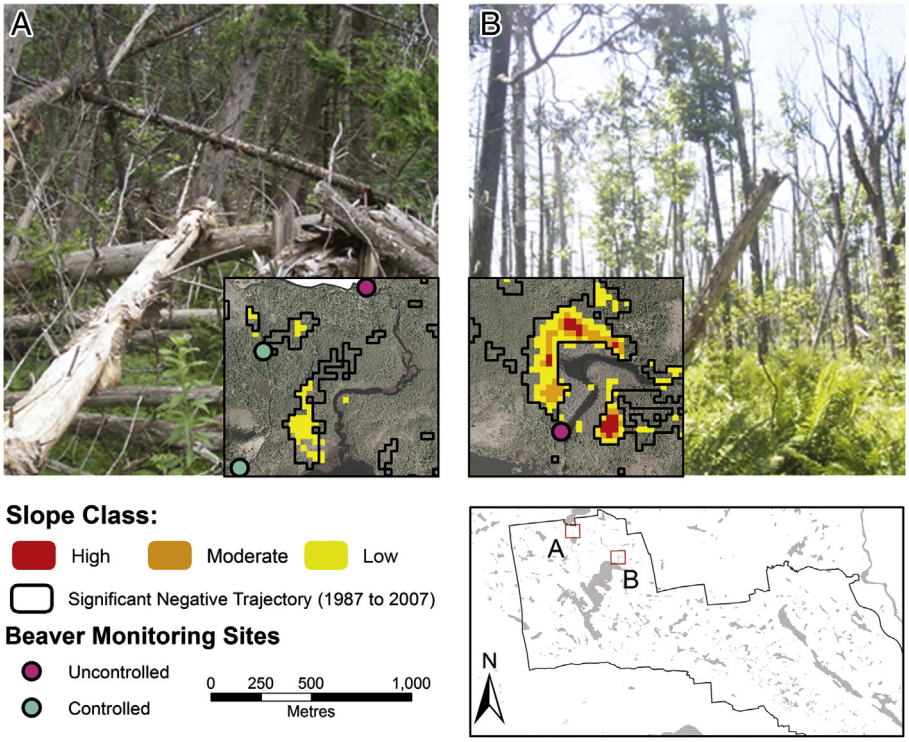

Fig. 6. Change maps and field photos of two known locations of deteriorating forests in Gatineau Park, showing the magnitude of the changes between 1987 and 2007 classified into three TS slope classes with respect to the TCW noise floor (NF): low (TS slope = 2 to 4 × NF), moderate (TS slope = 4 to 6 × NF) and high (TS slope > 6 × NF). Area A showed a low rate of change while Area B showed mostly high rates of change over the twenty year period. Both sites are in proximity to uncontrolled beaver monitoring sites and both are suffering from beaver-induced flooding. Photos: June 21 and June 22, 2010.

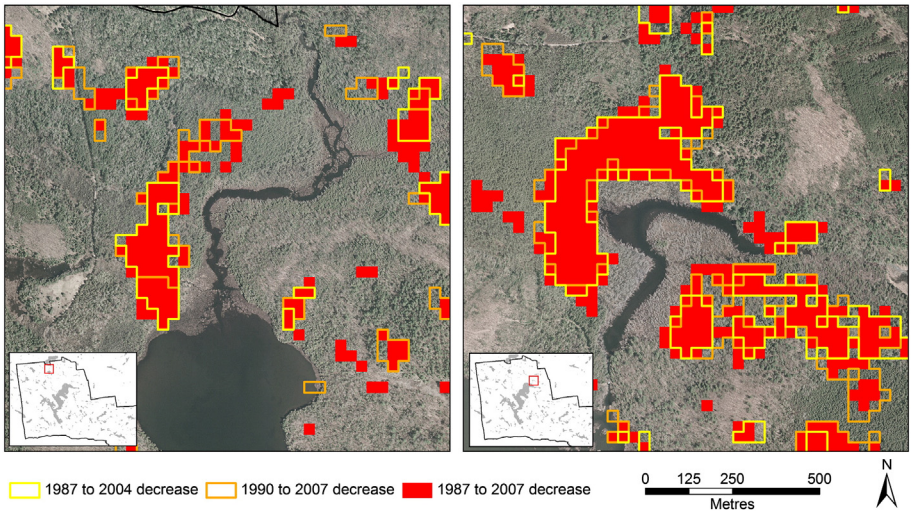

Fig. 7. Example areas in the northwest portion of Gatineau Park showing significant negative TCW trajectories for the 20- and 17-year time series.

suggested that very little change had occurred. Fig. 8 shows a sub-area of Gatineau Park, illustrating areas of both negative and positive TCW changes, for all three monitoring interval scenarios. Though the estimated areas of change are slightly different when using a 1–3 or 4–5 year monitoring interval, the locations targeted are quite similar. While the results of the 1–3 year interval are likely the most reliable, comparable results were achieved using a 4–5 year interval, a finding that is useful from a management perspective.

Overall, the results of the 20-year time series were deemed to be the most reliable, so they were used to assess the vegetation communities being impacted over this period. Table 3 shows that deciduous forests experienced the most areas with decreasing vegetation, while mixed forests had the most area with increasing vegetation. When considering the proportion of these changes in relation to the area represented by each functional group in the park, positive and negative change for coniferous forests is the most significant. Over 10% of the total area of coniferous forests was highlighted as declining, and over 4% was identified as growing. Mixed forests show higher proportional change than deciduous forests, for both change directions. Thus, deciduous forests, which comprise the largest area of the park, are more stable than mixed and coniferous forests.

3.2.2.4. Validation of detected negative and positive trends. Of the 30 randomly selected sites not used in model building that were identified

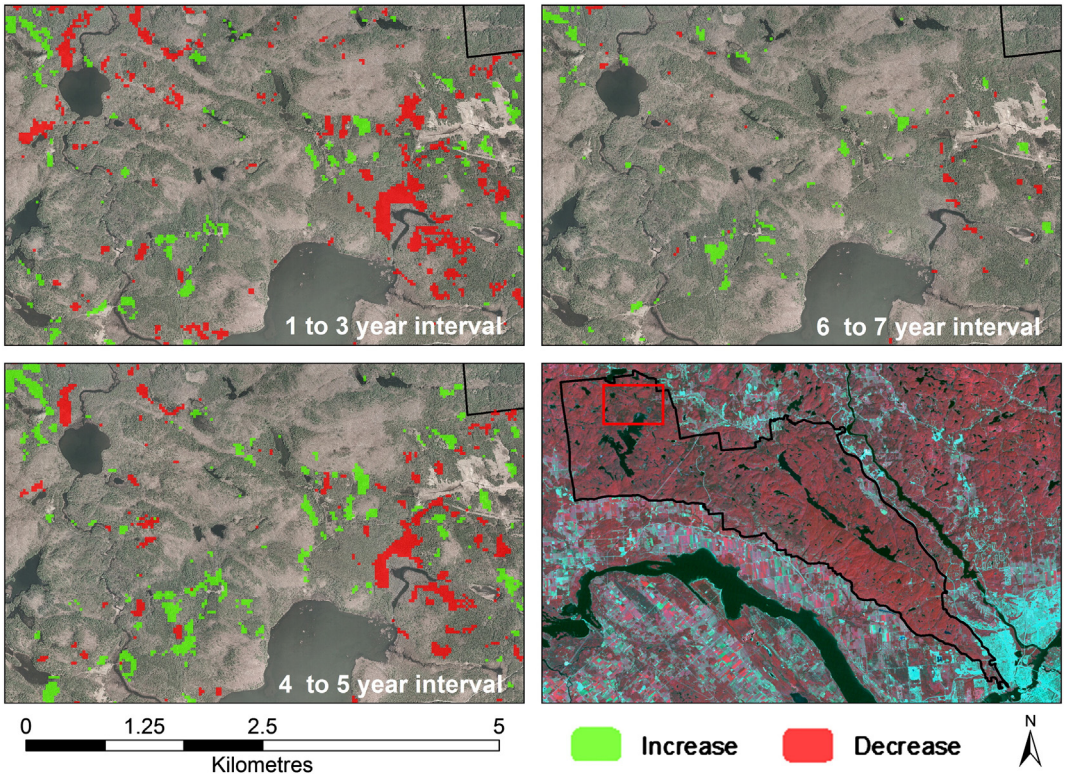

Fig. 8. Significant temporal trends in TCW (representing vegetation abundance), as represented by the CMK S-stat ($p \leq 0.05$) and TS slope greater than the noise floor for time series using 1–3, 4–5, and 6–7 year monitoring intervals. The bottom right map shows the area of the images (red outline) within Gatineau Park (black outline). (For interpretation of the references to color in this figure legend, the reader is referred to the web version of this article.)

Table 3
Summary of functional group trends between 1987 and 2007. The total area of change, as well as the proportion of change for each functional group is given.

Direction of TCW change	Total change area (ha)	Functional specific change (area and proportion of each class)					
		Conifer		Mixed		Deciduous	
		Area (ha)	% of class	Area (ha)	% of class	Area (ha)	% of class
Increase	434	61	4.4	216	2.5	157	0.8
Decrease	987	149	10.9	360	4.1	478	2.5

as undergoing significant negative TCW change in the 20-year trend analysis, 2011 visual field verification showed that 23 (77%) of them were clearly suffering forest decline with fallen trees, standing dead trees and thinned crown foliage. For 14 of these 23 sites, decline was occurring due to flooding or soil saturation. Another five sites were associated with portions of a plantation that were clearly growing very poorly. The remaining sites were difficult to categorize, but generally showed evidence of decline in the dominant overstory species. While seven of the sites could not be considered declining forests based on the single visit of 2011, four were undergoing a compositional change with younger deciduous trees beginning to reach the canopy heights of the more mature coniferous species. Based on the relationship in Fig. 2, an increasing proportion of deciduous species over time will also produce a negative TCW trajectory. This highlights the need for field verification of areas showing negative temporal trends in TCW to determine if they are related to physical conditions or successional species changes.

To investigate these results further, the TCW spectral trajectories of the validation sites were extracted, as represented by the average TCW for all pixels of each site for each year of the time series. Figs. 9–11 provide examples of independent validation sites that showed negative TCW change from 1987 to 2007. The site in Fig. 9 decreased in TCW by about 10 units during this time period, which, based on the relationship in Fig. 2, represents a decline in LAI of about 2. This seems realistic when viewed as a relative LAI change due to gradual flooding of the site. The photo in Fig. 9, taken in 2011, represents even further decline from 2007. Other sites with negative trajectories appeared to be undergoing changing canopy structure. These sites often included a relatively high proportion of standing dead trees and large canopy gaps (e.g., as in Fig. 10) and the slope of the TCW trend was not as steep as for sites such as in Fig. 9 that were undergoing more severe changes in hydrologic conditions.

Fig. 11 shows a unique condition within the validation set where dead and live trees were bent in the shape of an arc. This is typical of ice storm damage and these could be residual effects from the large storm of 1998. The area also exhibited saturated soils and may be undergoing gradual flooding. Based on the TCW trajectory in Fig. 11, decline was ongoing before the storm and continued after the storm. The storm's immediate effects are evident in the 1999 TCW value, which is markedly below the overall trend. Thus, the temporal dynamics for this area may be a combination of both abrupt and gradual changes due to different processes.

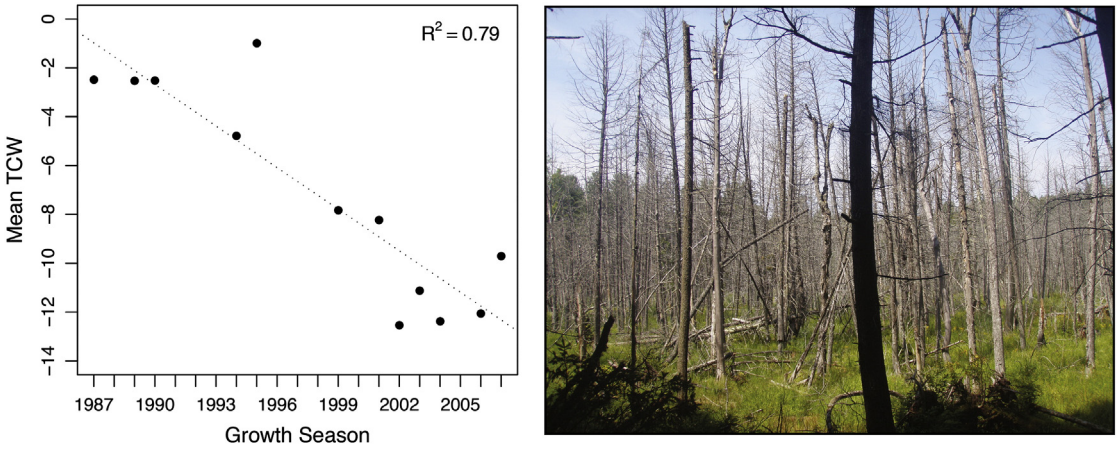

Fig. 9. Validation site showing decline due to local changes to surface water hydrology. Photo: August 17, 2011.

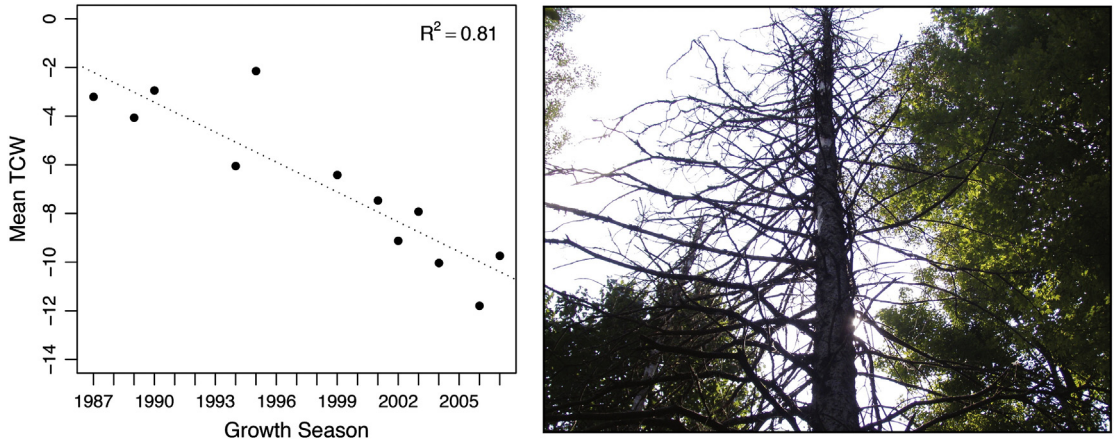

Fig. 10. Validation site showing decline in upper canopy trees, forming large canopy gaps. Photo: August 18, 2011.

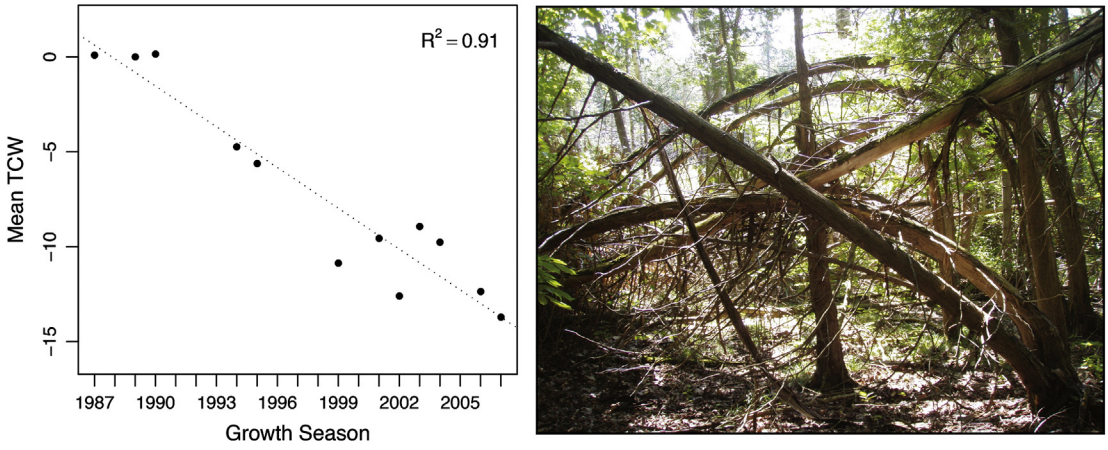

Fig. 11. Validation site showing a negative TCW trajectory associated with flooding, but punctuated by 1998 ice storm damage. Photo: August 19, 2011.

Of the 30 randomly selected sites not used in model building that were identified as undergoing significant positive change in the 20-year trend analysis, 2011 field verification showed 28 (93%) of them were clearly growing forests. Eight (27%) of these 28 sites were plantations, and the remaining 20 (66%) were in very early stages of forest succession. Although growth also occurs during mature stages of succession, the related TCW changes may be difficult to detect compared to the changes during early successional stages. Most plantations in the park are more than 20 to 30 years old and many were growing significantly during the 20-year time period and showed positive trends in TCW.

Figs. 12 and 13 provide examples of independent validation sites that showed positive TCW change from 1987 to 2007. Based on Fig. 1, the 35 year old plantation in Fig. 12 experienced an increase in LAI of about 2. In the early successional forest in Fig. 13, which had been a clearing for equipment storage and staging during construction of a nearby electrical power corridor, the most mature trees were about 30 years old and experienced an increase in LAI of about 4.

Overall, the field validation showed that the significant changes mapped using the 20-year time series were accurate, especially from a user's perspective as the field-validated errors of commission of the mapped changes were low. The CMK and TS trend analyses highlighted regions in the park that are indeed associated with changing forest conditions. The methods provide a cost effective and time efficient means for determining priority regions in the park, and for gaining a better understanding of the vegetation dynamics of such landscapes.

4. Discussion

4.1. Significant findings

This research showed that long-term trend analysis using a vegetation index such as TCW derived from a relatively calibrated Landsat image time series is a practical means to detect and map the location and magnitude of temporal dynamics of a forested landscape such as Gatineau Park. While the detailed results of this research are specifically applicable to Gatineau Park, the empirical modeling and remote sensing methods used and evaluated herein provide insights towards remote monitoring systems and ecosystem management for temperate humid environments. Prior to this research, several published works demonstrated the utility of a Landsat image time series for change detection (Coppin & Bauer, 1994, 1995; Song & Woodcock, 2003). Of the relevant studies, many focused on semi-arid coniferous forest environments, and/or in regions where forest change was quite drastic over the time period (Royle & Lathrop, 1997; Sonnenschein, Kuemmerle, Udelhoven, Stellmes, & Hostert, 2011; Vogelmann et al., 2009). Spectral reflectance in those environments is potentially very different than Gatineau Park, which is dominated by temperate deciduous species. We provide new information on potential use and capability of such methods in detection, mapping and monitoring of vegetation dynamics in such forests.

This research also provided a direct link between detected spectral change and field measured physical parameters such as LAI through the empirical models that were developed. This modeling approach is

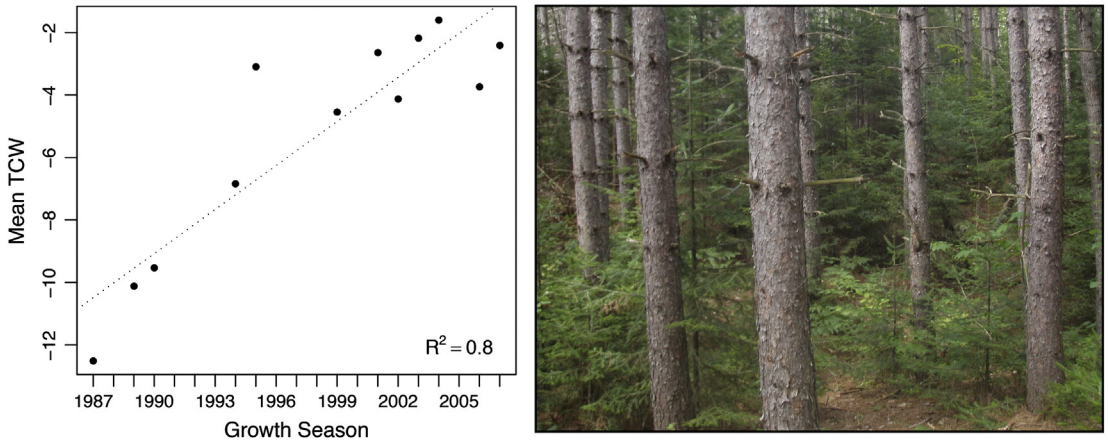

Fig. 12. Validation site showing a significant positive TCW trend associated with a young red pine plantation. Photo: August 16, 2011.

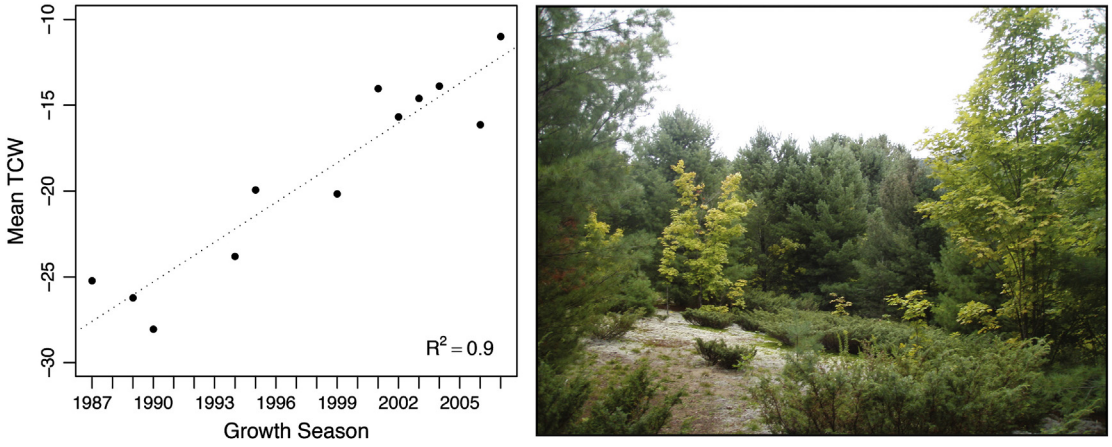

Fig. 13. Validation site showing a significant positive TCW trend associated with an early successional forest. Photo: August 16, 2011.

useful from an explanatory perspective and allowed for direct independent field validation with high certainty (Liu & Zhou, 2004). TCW was the most suitable image variable for mapping and monitoring vegetation abundance. It is mostly weighted (negatively) by the two Landsat short wave infrared bands (Table 1), which decrease in brightness (reflectance) as canopy moisture increases. However, it also includes moderate positive weighting of the NIR band and the red band, the latter having less influence on output values because vegetation brightness (reflectance) in the red is much lower than in the NIR or SWIR. Without field data, image variable selection is generally based on recommendations in the literature, which avoids time consuming field data collection but may result in less robust models that may not be reliable in the context of long term trend analysis. Our empirical methods also led to additional discoveries such as the conifer-specific relationship between TCW and average DBH of standing dead trees ($r = 0.84$). Although further work would be required, this relationship may be useful for mapping changing dead wood distributions (e.g., as conducted by Pasher and King (2009) in a small portion of the park, using other empirical methods applied to high resolution airborne imagery). Another such discovery was the strong and positive relationship between LAI and TCW ($r = 0.81$; Fig. 2). The interpretation of this relationship was extended over time such that increasing TCW detected in the time series could be interpreted as increasing LAI and vice versa. However, it must be noted that LAI dynamics are not only indicative of forest growth or decline, they may also be indicative of composition changes. The TCW–LAI relationship of Fig. 2 showed a distinct gradient among the functional forest groups. Deciduous forests generally had the lowest TCW and LAI (~2.5–6.2) while coniferous forests had the highest and also varied the most (LAI ~ 3.8–11.5), with mixed forests in between. In a few areas of the park, detected TCW trends were observed to be associated with such compositional changes over time as conifers were gradually growing in the understory of a deciduous canopy, or vice versa, where older plantations were deteriorating and deciduous understory was emerging. Thus, from a forest management perspective, TCW could be used as an indicator of vegetation structure, abundance and composition, and TCW trends may indicate changes in either quantity or composition, or both together. Such change mapping can be used in monitoring target areas for finer scale field analysis, thus significantly reducing the efforts required over a large area such as Gatineau Park.

In TCW trend analysis, the Theil–Sen slope estimate and Contextual Mann–Kendall significance test were found to be very clear indicators of significant change over a twenty year period. Not all studies report on the significance of change results, but these are essential components of any trend analyses (Neeti & Eastman, 2011). The spectral trajectories mapped in this research were considered to be statistically significant at the 95% confidence level, providing a distinct level of certainty to the analysis.

To test the sensitivity of the trend analysis results to the data set used, two tests were conducted. First, modifying the start and end years of the time series by dropping either the first or last years to produce two 17-year subsets did not have a significant effect on the trends detected. Areas of significant growth or decline were generally detected as accurately as in the full 20-year series but the spatial extent of detected areas of change varied amongst the three series. Second, modifying the monitoring interval of the image time series by dropping certain years to produce subset time series with 3–5 or 6–7 year intervals showed that change results for the 3–5 year interval were similar to those for the 1–3 year intervals of the full 20 year time series. Similarly, Lunetta, Johnson, Lyon, and Crotwell (2004) reported that a minimum monitoring frequency of 3 to 4 years is required for Landsat 5 TM time series ecosystem monitoring. They also stated a reduction in modeling errors could likely be achieved if the temporal frequency of the image time series was increased to 1 to 2 years. If larger intervals are used the time series must be longer in order to achieve an appropriate sample size for statistical analysis. While both the TS and CMK techniques are considered robust for small sample sizes, larger samples are generally considered more statistically reliable (Yue, Pilon, & Cavadias, 2002). The 6–7 year monitoring interval tested over 20 years in this study only had four observations and could not be compared with confidence to the shorter intervals evaluated. While tighter monitoring intervals are ideal, knowledge of a minimum monitoring frequency is important for forest and data management purposes.

Field validation of trends detected in the 20-year TCW time series (1987–2007) showed that growth trends were more accurately detected (93%) than forest decline trends (77%); this was purely based on an assessment of user's accuracy (i.e. field validation of detected TCW changes at 30 additional independent sites not used in modeling). It was more difficult to objectively assess producer's accuracy and errors of omission (i.e. changes that occurred that were not detected), since all field data acquired were used in the trend analysis.

4.2. Limitations and recommendations for future research

Like many optical remote sensing studies, this research was limited by the quality and availability of image data. Many Landsat scenes for Gatineau Park between 1984 and 2010 exhibited significant atmospheric effects, affecting not only the imagery over the park's forests, but also the stable targets (i.e. bright and dark PIFs) required for the calibration process that were 10 to 20 km outside the park. Thus, an image representing Gatineau Park under relatively clear skies could be considered unsuitable if atmospheric distortions in proximity to the park masked out these necessary targets for calibration. This limited the number of suitable scenes for trend analysis, but fortunately this research showed that gaps within an image time series can be as large

as 5 years without significantly affecting the reliability of the results. With Landsat trend analysis now common, progressive research will help to refine image pre-processing methods. The challenges for forest trend analysis in remote sensing include reducing the effects of the atmosphere, topography, phenology, and view angle (Song et al., 2002). Conversion of Landsat DN data to reflectance (Chander, Markham, & Helder, 2009) prior to deriving vegetation indices is becoming more common for large spatial data sets (Fraser, Olthof, Carrière, Deschamps, & Pouliot, 2011). Our tests of ATCOR2 calibration to surface reflectance did not produce as stable a time series as the PIF-based relatively calibrated series, and top-of-atmosphere (TOA) reflectance (Gómez et al., 2011), as derived using the coefficients in Chander et al. (2009), were very highly correlated with our Landsat brightness (DN) data. Some of these uncertainties are much more difficult to control for, and the ways they affect the signals received by a sensor are not spatially homogenous.

One approach to this issue could be to use other Landsat-based sensors such as the multispectral scanner (MSS) or Enhanced Thematic Mapper Plus (ETM+) to reduce data gaps in the image time series (Vogelmann et al., 2009). We opted to use data from only one sensor to control the data consistency, maintain as low a 'noise floor' as possible, and avoid the need for sensor to sensor calibration. However, for time series longer than the Landsat 5 TM archive or for time series including post Landsat 5 TM dates, use of multiple sensor data will be required. Landsat 8 will help alleviate this by maintaining relatively straightforward cross calibration with previous Landsat sensors. Alternatively, imagery from sensors with higher spatial resolution such as Worldview 1 and 2 could be utilized. This would provide for more spatial detail and perhaps more precise temporal analysis but multiple images would be required to cover the park (with associated cross calibration issues), the park has not acquired such imagery in the past, and the data are costly in comparison to the free Landsat archive, so a significant funding commitment would be required to develop a future temporal database with such data.

5. Conclusion

Using an empirical framework, detection and mapping of forest change in Gatineau Park, Québec was implemented using a Landsat 5 TM image time series. The methods used in this research provide means to feasibly and efficiently monitor forest dynamics within a single scene. With additional scene to scene calibration, they could be extended to a larger area represented by multiple scenes.

To address Objective 1, several vegetation indices and data transformations were selected based on their well-known theoretical and empirically proven representation of reflectance relationships with vegetation abundance. Empirical models of vegetation metrics developed for the forests of this study area were strong, indicating that the selected vegetation indices were good predictors of vegetation structure and quantity. In particular, Tasseled Cap Wetness (TCW) was the most robust index, responding to spatial and temporal variations in canopy moisture and greenness, and in turn providing a very strong relationship with LAI ($r = 0.81$) estimated from hemispherical photos. To address Objective 2, TCW was subsequently applied in time series trend analysis over a 20-year period, by combining the Theil–Sen trend slope estimate with the Contextual Mann–Kendall significance test. Statistically significant ($p \leqq 0.05$) trends that were greater than the noise floor were mapped over the study area forests. To address Objective 3, the resulting trend map was analyzed in various ways. Overall, the map showed that 1.5% and 2.7% of the park's forests had undergone statistically significant positive and negative change, respectively, in TCW and, by consequence, in vegetation abundance as represented by the TCW–LAI relationship. Field validation using 60 additional sample locations not applied in trend modeling showed the map to be 77% and 93% accurate in detection of forest decline and growth, respectively. Many of the areas found to be deteriorating were undergoing hydrologic changes and water inundation, resulting in gradual tree decline and mortality. Most areas experiencing growth were found to be younger forests that had been planted or had in-filled following disturbance in the previous decades. The empirical models of LAI against TCW and the detected TCW temporal trends also showed distinct differences between deciduous and coniferous species. Tests of the influence of the beginning and end years in the time series showed that the same trends were detected if either year was dropped from the series, but the extent of given change areas detected was generally contracted (smaller) in relation to the extent detected using the full 20 year time series. Tests of the effects of the interval between observation years showed that intervals of 3–5 years detected similar changes and change area extents but longer intervals of 6–7 years between observations were not as sensitive to temporal trends in the forests.

The methods evaluated in this study provide the ability to analyze and understand forest ecosystem dynamics. Given the low data cost and straightforward implementation procedures, such methods can be used in development of forest monitoring programs for land use management in Gatineau Park and other similar landscapes.

Acknowledgments

This research was funded by NSERC Discovery Grants to D. King and S. Mitchell. Data acquisition, processing and analysis were conducted in the Geomatics and Landscape Ecology Lab of Carleton University (http://www.glel.carleton.ca/), which is co-directed by King, Mitchell, L. Fahrig and K. Lindsay, and was funded by the Canada Foundation for Innovation, Ontario Innovation Trust, Hamlin Family Fund, Environment Canada, and Carleton University. The National Capital Commission provided access to Gatineau Park and facilitated the research development and implementation. The authors are very grateful for the assistance of Blair Kennedy, Sam Munoz, and Evan Seed in conducting the field research, and to Leanne Czerwinski for preparing the graphics.

References

Carson, T. N., & Ripley, D. A. (1997). On the relation between NDVI, fractional vegetation cover, and leaf area index. *Remote Sensing of Environment*, *62*, 241–252.
Chander, G., Markham, B.L., & Helder, D. L. (2009). Summary of current radiometric calibration coefficients for Landsat MSS, TM, ETM+, and EO-1 ALI sensors. *Remote Sensing of Environment*, *113*(5), 893–903.
Chavez, P.S., Jr. (1996). Image-based atmospheric corrections — Revisited and improved. *Photogrammetric Engineering and Remote Sensing*, *62*(9), 1025–1036.
Chen, J. M., & Cihlar, J. (1995). Plant canopy gap-size analysis theory for improving optical measurements of leaf area index. *Applied Optics*, *34*, 6211–6222.
Chen, J., Govind, A., Sonnentag, O., Zhang, Y., Barr, A., & Amiro, B. (2006). Leaf area index measurements at Fluxnet-Canada forest sites. *Agricultural and Forest Meteorology*, *140*, 257–268.
Chen, X., Vierling, L., & Deering, D. (2005). A simple and effective radiometric method to improve landscape change detection across sensors and across time. *Remote Sensing of Environment*, *98*, 63–79.
Chen, X., Vierling, L., Rowell, E., & DeFelice, T. (2004). Using lidar and effective LAI data to evaluate IKONOS and Landsat 7 ETM + vegetation cover estimates in a ponderosa pine forest. *Remote Sensing of Environment*, *91*, 14–26.
Coppin, P. R., & Bauer, M. E. (1994). Processing of multitemporal Landsat TM imagery to optimize extraction of forest cover change features. *IEEE Transactions on Geoscience and Remote Sensing*, *32*(4), 918–927.
Coppin, P. R., & Bauer, M. E. (1995). The potential contribution of pixel-based canopy change information to stand-based forest management in the northern U.S. *Journal of Environmental Management*, *44*(1), 69–82.
Crist, E. P. (1985). Short communication: A TM Tasseled Cap equivalent transformation for reflectance factor data. *Remote Sensing of Environment*, *17*, 301–306.
Crist, E. P., & Cicone, R. C. (1984). A physically-based transformation of Thematic Mapper data—The TM Tasseled Cap. *IEEE Transactions on Geoscience and Remote Sensing*, *GE-22*(3), 256–263.
Czerwinski, C. (2012). *Forest change detection and mapping in Gatineau Park, Québec, 1987–2010 using Landsat imagery.* : Carleton University (Unpublished master's thesis).
Du, Y., Philippe, M., & Cihlar, J. (2002). Radiometric normalization of multitemporal high-resolution satellite images with quality control for land cover change detection. *Remote Sensing of Environment*, *82*(1), 123–134.
Fraser, R. H., Olthof, I., Carrière, M., Deschamps, A., & Pouliot, D. (2011). Detecting long-term changes to vegetation in northern Canada using the Landsat satellite image archive. *Environmental Research Letters*, *6*(4) (http://iopscience.iop.org/1748-9326/6/4/045502/)

Gómez, C., White, J., & Wulder, M. (2011). Characterizing the state and process of change in a dynamic forest environment using hierarchical spatio-temporal segmentation. *Remote Sensing of Environment*, *115*(7), 1665–1679.
Goward, S. N., Markham, B., Dye, D.G., Dulaney, W., & Yang, J. (1991). Normalized difference vegetation index measurements from advanced very high resolution radiometer. *Remote Sensing of Environment*, *35*, 257–277.
Gower, S. T., Kucharik, C. J., & Norman, J. M. (1999). Direct and indirect estimation of leaf area index, f_{APAR}, and net primary production of terrestrial ecosystems. *Remote Sensing of Environment*, *70*, 29–51.
Hall, R., Davidson, D., & Peddle, D. (2003). Ground and remote estimation of leaf area index in Rocky Mountain forest stands, Kananaskis, Alberta. *Canadian Journal of Remote Sensing*, *29*, 411–427.
He, L., Chen, J. M., Zhang, S., Gomez, G., Pan, Y., McCullough, K., et al. (2011). Normalized algorithm for mapping and dating forest disturbances and regrowth for the United States. *International Journal of Applied Earth Observation and Geoinformation*, *13*(2), 236–245.
Healey, S. P., Cohen, W., Zhiqiang, Y., & Krankina, O. (2005). Comparison of Tasseled Cap-based Landsat data structures for use in forest disturbance detection. *Remote Sensing of Environment*, *97*, 301–310.
Hoaglin, D., Mosteller, F., & Tukey, J. (2000). *Understanding Robust and Exploratory Data Analysis (285–294)*. New York: John Wiley.
Huete, A.R. (1988). A soil-adjusted vegetation index (SAVI). *Remote Sensing of Environment*, *25*, 295–309.
Huete, A.R., Liu, H. Q., Batchily, K., & van Leeuwen, W. J.D. (1997). A comparison of vegetation indices over a global set of TM images for EOS-MODIS. *Remote Sensing of Environment*, *59*, 440–451.
Jiang, Z., Huete, A.R., Didan, K., & Miura, T. (2008). Development of a two-band enhanced vegetation index without a blue band. *Remote Sensing of Environment*, *112*(10), 3833–3845.
Jin, S., & Sader, S. A. (2005). Comparison of time series tasseled cap wetness and the normalized difference moisture index in detecting forest disturbances. *Remote sensing of Environment*, *94*, 364–372.
Kaiser, H. F. (1958). The varimax criterion for analytic rotation in factor analysis. *Psychometrika*, *23*(24), 187–200.
Kaiser, H. F. (1960). The application of electronic computers to factor analysis. *Educational and Psychological Measurement*, *20*(1), 141–151.
King, D. J., Olthof, I., Pellikka, P. K. E., Seed, E., & Butson, C. (2005). Modelling and mapping damage to forests from an ice storm using remote sensing and environmental data. *Natural Hazards*, *35*, 321–342.
Leblanc, S. G., & Chen, J. M. (2001). A practical scheme for correcting multiple scattering effects on optical LAI measurements. *Agricultural and Forest Meteorology*, *110*, 125–139.
Leblanc, S. F., Chen, J. M., Fernandes, R., Deering, D. W., & Conley, A. (2005). Methodology comparison for canopy structure parameters extraction from digital hemispherical photography in boreal forests. *Agricultural and Forest Meteorology*, *129*, 187–207.
Liu, H., & Zhou, Q. (2004). Accuracy analysis of remote sensing change detection by rule-based rationality evaluation with post-classification comparison. *International Journal of Remote Sensing*, *25*(5), 1037–1050.
Louis, H. (2008). *Insectes et Maladies des Arbres du Québec Rapport Annuel 2008 Secteur 71 — Unités de Gestion de la Coulonge et de la Basse-Lièvre (1–37)*. : Ministère des ressources naturelles et de la Faune du Québec.
Lunetta, R. S., Johnson, D.M., Lyon, J. G., & Crotwell, J. (2004). Impacts of imagery temporal frequency on land-cover change detection monitoring. *Remote Sensing of Environment*, *89*, 444–454.
Myeong, S., Nowak, D. J., & Duggin, M. J. (2006). A temporal analysis of urban forest carbon storage using remote sensing. *Remote Sensing of Environment*, *101*, 277–282.
National Capital Commission. (NCC) (2005). Gatineau Park Master Plan. http://www.canadascapital.gc.ca/sites/default/files/pubs/NCC-Gatineau-Park-Master-Plan-2005.pdf
Neeti, N., & Eastman, J. (2011). Contextual Mann-Kendall approach for the assessment of trend significance in image time series. *Transactions in GIS*, *15*(5), 599–611.
Paolini, L., Grings, F., Sobrinos, J. A., Munoz, J. C., & Karszenbaum, H. (2006). Radiometric correction effects in Landsat multi-date/multi-sensor change detection studies. *International Journal of Remote Sensing*, *27*(4), 685–704.
Pasher, J., & King, D. J. (2009). Mapping dead wood distribution in a temperate hardwood forest using high resolution airborne imagery. *Forest Ecology and Management*, *258*, 1536–1548.
Pasher, J., & King, D. J. (2010). Multivariate forest structure modelling and mapping using high resolution airborne imagery and topographic information. *Remote Sensing of Environment*, *114*, 1718–1732.
Pasher, J., & King, D. J. (2011). Development of a forest structural complexity index based on multispectral airborne remote sensing and topographic data. *Canadian Journal of Forest Research*, *41*, 44–58 (IUFRO Special Issue on Extending Forest Inventory and Monitoring over Space and Time).
Pettorelli, N., Vik, J. O., Mysterud, A., Gaillard, J. -M., Tucker, C. J., & Stenseth, N. C. (2005). Using the satellite-derived NDVI to assess ecological responses to environmental change. *Trends in Ecology & Evolution (Personal Edition)*, *20*(9), 503–510.
Pisaric, M. F. J., King, D. J., MacIntosh, A. J. M., & Bemrose, R. (2008). Impact of the 1998 ice storm on the health and growth of sugar maple (Acer saccharum Marsh.) dominated forests in Gatineau Park, Québec. *The Journal of the Torrey Botanical Society*, *135*(4), 530–539.
Powell, S. L., Cohen, W. B., Healey, S. P., Kennedy, R. E., Moisen, G. G., Pierce, K. B., et al. (2010). Quantification of live aboveground forest biomass dynamics with Landsat time series and field inventory data: A comparison of empirical modeling approaches. *Remote Sensing of Environment*, *114*, 1053–1068.
Richter, R. (1990). A fast atmospheric correction algorithm applied to Landsat TM images. *International Journal of Remote Sensing*, *11*(1), 159–166.
Royle, D., & Lathrop, R. (1997). Monitoring hemlock forest health in New Jersey using Landsat TM data and change detection techniques. *Forest Science*, *43*(3), 327–335.
Schlagel, J.D., & Newton, C. M. (1996). A GIS-based statistical method to analyze spatial change. *Photogrammetric Engineering and Remote Sensing*, *62*(7), 839–844.
Schott, J. R., Salvaggio, C., & Volchok, W. J. (1988). Radiometric scene normalization using pseudoinvariant features. *Remote Sensing of Environment*, *26*(1), 1–6.
Schroeder, T. A., Cohen, W. B., Song, C., Canty, M. J., & Yang, Z. (2006). Radiometric correction of multi-temporal Landsat data for characterization of early successional forest patterns in western Oregon. *Remote Sensing of Environment*, *103*, 16–26.
Seed, E. D., & King, D. J. (2003). Shadow brightness and shadow fraction relations with effective leaf area index: Importance of canopy closure and view angle in mixedwood boreal forest. *Canadian Journal of Remote Sensing*, *29*(3), 324–335.
Sen, P. K. (1968). Estimates of the regression coefficient based on Kendall's tau. *Journal of the American Statistical Associated*, *63*(324), 1379–1389.
Song, C., & Woodcock, C. E. (2003). Monitoring forest succession with multitemporal Landsat images: Factors of uncertainty. *IEEE Transactions on Geoscience and Remote Sensing*, *41*(11), 2557–2567.
Song, C., Woodcock, C. E., & Li, X. (2002). The spectral/temporal manifestation of forest succession in optical imagery — The potential of multitemporal imagery. *Remote Sensing of Environment*, *82*(2), 285–302.
Song, C., Woodcock, C. E., Seto, K., Lenney, M., & Macomber, C. (2001). Classification and change detection using Landsat TM data: When and how to correct for atmospheric effects? *Remote Sensing of Environment*, *75*, 230–244.
Sonnenschein, R., Kuemmerle, T., Udelhoven, T., Stellmes, M., & Hostert, P. (2011). Differences in Landsat-based trend analyses in drylands due to the choice of vegetation estimate. *Remote Sensing of Environment*, *115*, 1408–1420.
Spies, T. A. (1998). Forest structure: A key to the ecosystem. *Northwest Science*, *72*(2), 34–39.
Theil, H. (1950). A rank-invariant method of linear and polynomial regression analysis I, II and III. *Proceedings, Koninklijke Nederlandse Academie van Wetenschappen*, *53*. (pp. 386–392) (521-525, 1397-1412).
Torontow, V., & King, D. J. (2012). Forest complexity modelling and mapping with remote sensing and topographic data: comparison of three methods. *Canadian Journal of Remote Sensing*, *37*(4), 387–402.
Turner, D. P., Cohen, W. B., Kennedy, R. E., Fassnacht, K. S., & Briggs, J. M. (1999). Relationships between leaf area index and Landsat TM spectral vegetation indices across three temperate zone sites. *Remote Sensing of Environment*, *70*(1), 52–68.
Vogelmann, J. E., Tolk, B., & Zhu, Z. (2009). Monitoring forest changes in the southwestern United States using multitemporal Landsat data. *Remote Sensing of Environment*, *113*(8), 1739–1748.
Wang, Q., Adiku, S., Tenhunen, J., & Granier, A. (2005). On the relationship of NDVI with leaf area index in a deciduous forest site. *Remote Sensing of Environment*, *94*, 244–255.
Yue, S., Pilon, P., & Cavadias, G. (2002). Power of the Mann-Kendall and Spearman's rho tests for detecting monotonic trends in hydrological series. *Journal of Hydrology*, *259*(1–4), 254–271.